Available online at www.sciencedirect.com
ScienceDirect
Polymer 48 (2007) 6056–6063
polymer
www.elsevier.com/locate/polymer

Nitrile butadiene rubber/hindered phenol nanocomposites with improved strength and high damping performance

Xiu-Ying Zhao [a], Ping Xiang [b], Ming Tian [a,c], Hao Fong [c,*], Riguang Jin [a], Li-Qun Zhang [a,b,**]

[a] The Key Laboratory of Beijing City on Preparation and Processing of Novel Polymer Materials, Beijing University of Chemical Technology, Beijing 100029, China
[b] The Key Laboratory for Nanomaterials, China Ministry of Education, Beijing University of Chemical Technology, Beijing 100029, China
[c] Department of Chemistry, South Dakota School of Mines and Technology, Rapid City, SD 57701, USA

Received 10 May 2007; received in revised form 3 August 2007; accepted 3 August 2007
Available online 9 August 2007

Abstract

A hindered phenol (AO-80) was studied to prepare rubber nanocomposites with nitrile butadiene rubber (NBR). The NBR/AO-80 rubber nanocomposites were successfully developed by applying the adopted preparation procedure/conditions, especially by introducing mechanical kneading of the NBR/AO-80 composites at a temperature higher than the melting point of AO-80, followed by the crosslinking of NBR molecules during the subsequent hot-pressing/vulcanization process. The nanocomposites consisted of two phases: (1) the AO-80 enriched phase (nanoparticles with the average size of approximately 20 nm) and (2) the NBR enriched phase (matrix). The generation and uniform distribution of the nanoparticles were attributed to the high temperature mechanical kneading process, the strong intermolecular interactions between AO-80 and NBR molecules, and the formation of a three-dimensional NBR network. The morphological, structural and mechanical properties of the composites were systematically investigated in each preparation step using SEM, TEM, DSC, XRD, FT-IR, DMTA and a tensile tester. The results indicated that the prepared NBR/AO-80 rubber nanocomposites had single relaxation transitions, improved tensile strengths, high dynamic mechanical loss values, and reasonably good stabilities. The NBR/AO-80 rubber nanocomposites are expected to have important applications as a high performance damping material.

Keywords: Nanocomposites; NBR; Hindered phenol

1. Introduction

The research on rubber nanocomposites can be both fundamental and applied, and has attracted growing attentions. Numerous studies have demonstrated that the uniform distribution of nano-scaled filler particles into a rubber matrix, with reasonably good interfacial bonding strength, could lead to a rubber nanocomposite with significantly improved properties [1–5]. For example, by distributing 10 phr (parts per hundred of rubber by mass) of organically modified montmorillonite into styrene butadiene rubber (SBR), the tensile strength of the resulting rubber nanocomposite could exceed 18 MPa, which was 9 times higher than that of the neat SBR [2]. It was also reported that when the particle size of magnesium hydroxide ($Mg(OH)_2$) was reduced from micron-level to nano-level, both the mechanical and the fire retardation properties of its filled ethylene propylene diene monomer (EPDM) rubber could be substantially improved [6]. Theoretical analyses have suggested that properties of nanofiller particles, interfacial bonding strength of filler/matrix, and uniform distribution of nanofiller particles were the most important factors on the properties of rubber nanocomposites [7–9].

Nanofillers can be generally classified as inorganic and organic ones. Inorganic nanofillers (including nano-scaled

* Corresponding author. Tel.: +1 605 3941229; fax: +1 605 394 1232.
** Corresponding author. The Key Laboratory of Beijing City on Preparation and Processing of Novel Polymer Materials, Beijing University of Chemical Technology, Beijing 100029, China. Tel.: +86 10 64434860; fax: +86 10 64433964.
E-mail addresses: hao.fong@sdsmt.edu (H. Fong), zhanglq@mail.buct.edu.cn (L.-Q. Zhang).

0032-3861/$ - see front matter © 2007 Elsevier Ltd. All rights reserved.
doi:10.1016/j.polymer.2007.08.011

carbon black, silica/silicate and metal oxide/hydroxide) have been extensively researched for decades, while organic nanofillers have been of increasing interests recently, particularly in the development of rubber nanocomposites. Unlike inorganic nanofillers that often require additional surface treatments to improve the filler/matrix interfacial properties, organic nanofillers usually possess favorable surface functional groups that can form strong intermolecular interactions (hydrogen bonding and/or van der Waals' forces) with the rubber molecules in the matrices. On the other hand, unlike most inorganic nanofillers that pre-exist as nano-scaled particles, organic nanofillers usually must be transformed into nano-scaled particles during the preparation of rubber nanocomposites. Therefore, effectively generating organic nanofiller particles and uniformly distributing them into rubber matrices are two major challenges during the preparation of rubber nanocomposites.

A hindered phenol of 3,9-bis[1,1-dimethyl-2-{β-(3-tert-butyl-4-hydroxy-5-methylphenyl)propionyloxy}ethyl]-2,4,8,10-tetraoxaspiro-[5,5]-undecane (AO-80) was investigated to prepare the rubber nanocomposites in this study. The chemical structure of AO-80 is shown in Fig. 1. The AO-80 molecule has a relatively high molecular weight, and AO-80 can be crystalline or amorphous, depending upon the processing procedures/conditions [10]. Nano-scaled particles containing amorphous AO-80 can be generated in the rubber matrices by mechanically kneading AO-80 with a polar rubber such as nitrile butadiene rubber (NBR) at a temperature higher than the AO-80 melting point of 122.5 °C, followed by hot-pressing/vulcanization. Additionally, since the AO-80 molecule has numerous polar functional groups (hydroxyl, carbonyl and others) that can form strong intermolecular interactions with NBR, the NBR/AO-80 rubber nanocomposites are likely to possess good filler/matrix interfacial properties. Wu and co-workers reported that AO-80 was used to prepare composites with chlorinated polyethylene (CPE) [11–13]. The preparation method that was adopted in their studies included: (1) adding various amounts of AO-80 (crystalline powder) into the pre-kneaded CPE, followed by kneading the mixtures at room temperature for 10 min; (2) heating the samples to a temperature higher than the melting point of AO-80 for 3 min, then hot-pressing the samples at 160 °C for 7 min at a pressure of 18 MPa; and (3) quenching the samples using an ice water bath to obtain the CPE/AO-80 composites. In their prepared composites, a small portion of the AO-80 existed as nanoparticles with sizes smaller than 100 nm, but the majority existed as particles with sizes of 0.4–0.5 μm. Such composites exhibited two distinct relaxation transitions: (1) the glass transition associated with CPE in the matrix and (2) the hydrogen bonding dissociation associated with AO-80 in the particles. While the authors discovered that hot-pressing was crucial for the formation of uniformly distributed AO-80 particles, the prepared composites could not be considered to be ''nanocomposites''. They also reported that the composites possessed a much higher dynamic mechanical loss property when compared to the neat CPE. This was attributed to the strong intermolecular interactions between the AO-80 and the CPE molecules, since such interactions would enhance the intermolecular friction and result in a large consumption of energy during dynamic deformations.

The aim of this study was to prepare, characterize and evaluate NBR/AO-80 composites with particle sizes that are smaller than 100 nm (nanocomposites). NBR is easier to crosslink/vulcanize than CPE since NBR contains butadiene units. More importantly, NBR can form stronger intermolecular interactions with AO-80 since the nitrile group in NBR has a higher polarity than the chlorine/carbon and α-hydrogen/carbon bonds in CPE. Unlike Wu and co-workers, we introduced two important steps into the preparation procedure: (1) high temperature (135 °C) kneading of NBR/AO-80 composites (note that Wu and co-workers simply heated their composites before conducting hot-pressing), and (2) molecularly crosslinking of NBR molecules during the subsequent hot-pressing/vulcanization process. Our hypotheses were that: (1) the mechanical kneading at a temperature higher than the melting point of AO-80 could molecularly disperse AO-80 into NBR. This was because the extensive shearing involved in the high temperature kneading process could greatly enhance the intermolecular interactions between the liquid state AO-80 and the rubbery state NBR molecules; and (2) the subsequent hot-pressing/vulcanization and its resulting formation of a three-dimensional NBR network could compress and aggregate the molecularly dispersed AO-80 into nano-scaled particles. The NBR network could also partially block the generated nanoparticles and effectively prevent them from over aggregation into large particles, thus could lead to the formation of NBR/AO-80 rubber nanocomposites. We adopted the following preparation method: (1) adding various amounts of AO-80 (crystalline powder) into the pre-kneaded NBR by applying a room temperature kneading process; (2) kneading the prepared NBR/AO-80 composites at a temperature higher than the melting point of AO-80; (3) after the high temperature kneaded samples being gradually cooled to room temperature, adding the compounding and crosslinking agents into the samples by applying a room temperature kneading process; (4) hot-pressing the samples at 160 °C to allow the NBR molecules to crosslink/vulcanize into three-dimensional rubbery networks; and (5) gradually cooling the hot-pressed/vulcanized samples to room temperature to prepare the final NBR/AO-80 composites (rubber nanocomposites). The

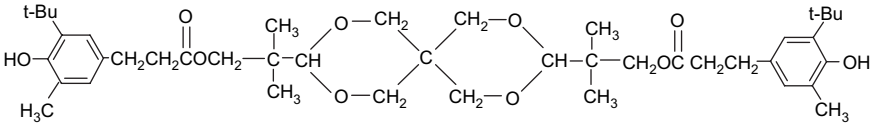

Fig. 1. Molecular structure of AO-80.

morphological and structural properties of the NBR/AO-80 rubber composites in each preparation stage were systematically investigated, and the static and dynamic mechanical properties of the composites were evaluated. The results indicated that NBR/AO-80 rubber nanocomposites were successfully prepared by applying the method described above. The nanocomposites exhibited single relaxation transitions, improved tensile strengths, excellent elastic recovery properties, and high dynamic mechanical loss values. The NBR/AO-80 rubber nanocomposites are expected to have important applications as a high performance damping material.

2. Experimental

2.1. Materials

NBR (N220S) with the acrylonitrile mass fraction of 41% was provided by Japan Synthetic Rubber Co., Ltd. (Tokyo, Japan). AO-80 (ADK-ATAB-AO-80), in the form of crystalline powder, was provided by Asahi Denka Co., Ltd. (Tokyo, Japan). Other chemicals and ingredients were purchased in China. All materials were used without further purification.

2.2. Sample preparation

NBR/AO-80 rubber composites were prepared using the following procedure/conditions: (1) after the as-received NBR was kneaded on a Φ152.4 mm two-roll mill at room temperature for 3 min, AO-80 (crystalline powder) was added with the NBR/AO-80 mass ratios of 100/0, 100/20, 100/40, 100/60, and 100/100. These mixtures were then kneaded at room temperature for 5 min to prepare the first-stage NBR/AO-80 composites (termed as NBR/AO-80a composites). (2) The NBR/AO-80a composites were then kneaded on the two-roll mill at 135 °C for 5 min and then gradually cooled to room temperature to prepare the NBR/AO-80b composites. (3) The NBR/AO-80b composites were then blended with compounding and crosslinking additives, including 5.0 phr ZnO, 2.0 phr stearic acid, 0.5 phr dibenzothiazole disulfide, 0.5 phr diphenyl guanidine, 0.2 phr tetramethylthiuram disulfide and 2.0 phr sulfur; the mixtures were then kneaded on the two-roll mill at room temperature for 10 min. (4) Finally, the mixtures were hot-pressed and crosslinked/vulcanized at 160 °C under the pressure of 15 MPa for varied periods of time, and then naturally cooled down to room temperature to prepare NBR/AO-80c composites. The amount of time used for the hot-pressing/vulcanization was pre-determined for each composite (each with different NBR/AO-80 mass ratios) using a disc rheometer (P355C2) purchased from Huanfeng Chemical Technology and Experimental Machine Co. (Beijing, China).

2.3. Analysis and characterization

The morphological, structural and mechanical properties of the NBR/AO-80 composites were systematically characterized/evaluated at each preparation stage using SEM, TEM, DSC, XRD, FT-IR, DMTA and a tensile tester. SEM images were taken from the representative fracture surfaces of the composites using an XL-30 field emission SEM made by FEI Co. in USA. The SEM specimens were prepared by fracturing the composites in liquid nitrogen. An H-800 TEM made by Hitachi, Ltd. in Japan was employed to examine the morphology and distribution of nanoparticles in the NBR/AO-80c nanocomposites. The TEM specimens of the NBR/AO-80c nanocomposites were prepared by cryogenic microtoming using a Reichert–Jung Ultracut Microtome and mounted on 200 mesh copper grids. DSC measurements were performed on a DSC 204F1 calorimeter made by Netzsch Co. in Germany. The DSC curves were recorded from −60 °C to 150 °C at an increasing temperature rate of 10 °C/min. XRD data were acquired from a Rigaku D/Max 2500VBZt/PC X-ray diffractometer made by Rigaku Corporation in Japan. The XRD data were recorded in the scattering angle range from 3° to 90°. Infrared measurements were conducted on a Nicolet 8700 FT-IR spectrometer made by Thermo Co. in USA. The FT-IR spectra were acquired by scanning the specimens in the wavenumber range from 400 cm^{-1} to 4000 cm^{-1} for 128 times with a resolution of 2 cm^{-1}. The FT-IR spectra of AO-80 (including both as-received and quenched AO-80) were acquired by using ultra-thin disk specimens pressed from AO-80 and anhydrous potassium bromide (KBr). The FT-IR spectra of NBR/AO-80 composites were acquired from film specimens with a thickness of approximately 1 mm, using the Attenuated Total Reflection (ATR) technique. Dynamic viscoelasticity measurements were carried out on a Dynamic Mechanical Thermal Analyzer (DMTA) made by Rheometric Scientific Co., Ltd. in USA. The dimensions of the DMTA specimens were 20 mm long, 6 mm wide and 1 mm in thickness. The temperature dependence of the dynamic tensile module was measured in the range from −60 °C to 150 °C with a frequency of 1 Hz and a heating rate of 3 °C/min. Tensile tests of the NBR/AO-80 composites were conducted according to ASTM standard (D412: dumbbell-shaped), and the specimens were tested on a LRX Plus Tensile Tester made by Lloyd instruments, Ltd. in UK.

3. Results and discussion

3.1. Morphology of NBR/AO-80 composites

The representative fracture surfaces of the prepared composites with the NBR/AO-80 mass ratio of 100/60 (termed as NBR/AO-80 (100/60) composites) are shown in Fig. 2. In the NBR/AO-80 (100/60)a composite (Fig. 2A), AO-80 existed primarily as micron-sized particles, and the particle size distribution was large. It also appeared that the interfacial bonding between AO-80 particles and NBR matrix was not strong, since numerous voids/holes were presented on the fracture surface. These voids/holes were generated by the dislodgement of the AO-80 particles during fracturing of the specimen. Fig. 2A suggests that the room temperature kneading could not sufficiently disperse AO-80 into NBR, and the

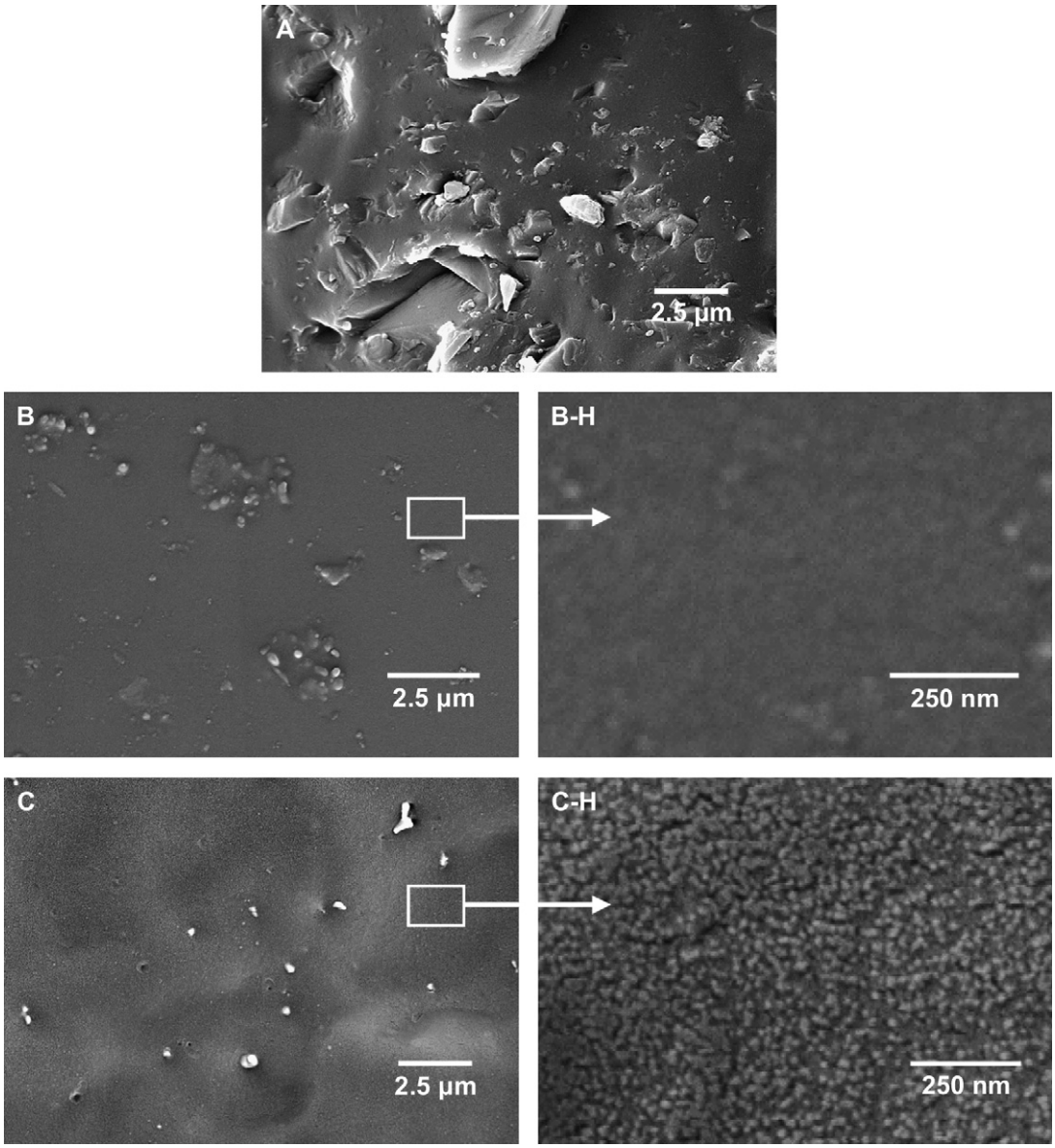

Fig. 2. SEM images of the representative fracture surfaces of (A) NBR/AO-80 (100/60)a, (B and B-H) NBR/AO-80 (100/60)b and (C and C-H) NBR/AO-80 (100/60)c composites.

NBR/AO-80a composites were micro-composites instead of nanocomposites.

After the NBR/AO-80 (100/60)a composite was mechanically kneaded at 135 °C (a temperature higher than the AO-80 melting point of 122.5 °C) for 5 min and then gradually cooled to room temperature, the NBR/AO-80 (100/60)b composite was obtained, and its representative fracture surface is shown in Fig. 2B and B-H (the high magnification image of a small area in Fig. 2B). The fracture surface of the NBR/AO-80 (100/60)b composite was much smoother than that of the NBR/AO-80 (100/60)a composite. Very few voids/holes could be identified by the microscope. Fig. 2B and B-H suggests that the mechanical kneading of NBR/AO-80a composites above the melting temperature of AO-80 would adequately mix AO-80 with NBR; the AO-80 in NBR/AO-80b composites might exist mainly as tiny nanoparticles (sizes of a few nanometers) or even as molecules/clusters. We believe that the extensive shearing associated with the high temperature mechanical kneading process could significantly promote the molecular-level mixing of liquid state AO-80 molecules and rubbery state NBR molecules. Intriguingly, the subsequent cooling did not cause any evident phase separation, probably due to the strong intermolecular interactions between AO-80 and NBR molecules. Therefore, NBR/AO-80b composites can be considered as molecular composites. This assumption is further supported by the DSC, XRD and DMA results. It is noted, however, that since the NBR/AO-80b composites were not crosslinked/vulcanized, their mechanical properties (especially strength) were low.

After the NBR/AO-80 (100/60)b composite was mixed with compounding/crosslinking additives, hot-pressed and crosslinked/vulcanized at 160 °C and then cooled to room

temperature, the NBR/AO-80 (100/60)c composite was prepared. The representative fracture surface of the NBR/AO-80 (100/60)c composite is shown in Fig. 2C and 2C-H (the high magnification image of a small area in Fig. 2C). Similar to that of the NBR/AO-80 (100/60)b composite, the fracture surface of the NBR/AO-80 (100/60)c composite was also smooth with no microscopically identifiable voids/holes. Energy dispersive spectrometer (EDS) attached to the SEM indicated that the particles in Fig. 2C were actually made of ZnO (a rubber compounding additive). Unlike that of the NBR/AO-80 (100/60)b composite, the fracture surfaces of the NBR/AO-80 (100/60)c composite were covered by nanoparticles with an average size of approximately 20 nm (Fig. 2C). During the hot-pressing/vulcanization process, the NBR/AO-80c composites with crosslinked NBR networks were developed. We believe that the three-dimensional rubbery network could compress and aggregate the molecularly dispersed AO-80 into nano-scaled particles; the network could also partially block the generated nanoparticles and effectively prevent them from over aggregation into large particles. Thus, the NBR/AO-80c composites were indeed nanocomposites.

Fig. 3 shows a representative TEM image of the NBR/AO-80 (100/60)c nanocomposite. The dispersed particles with sizes in the range from tens to hundreds of nanometers could be over-aggregated AO-80 particles, but are more likely ZnO particles. Although the average particle size of the as-received ZnO powder was much larger, we believe the mechanically kneading process could reduce the ZnO particle size. Furthermore, in the TEM images, the (transmitted electron density) difference between the AO-80 nanoparticles (which were actually AO-80 enriched phases containing amorphous AO-80 and some NBR chain segments, as discussed in the following section) and the NBR matrix (which was actually an NBR enriched phase with some molecularly dispersed AO-80) was slight, especially if the size of AO-80 nanoparticles was 20 nm or less.

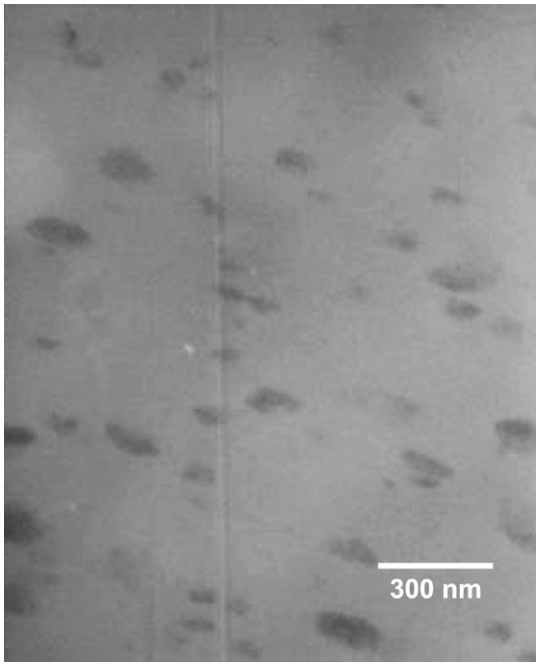

Fig. 3. Representative TEM image of the NBR/AO-80 (100/60)c composite.

3.2. Crystallization and glass transition of NBR/AO-80 composites

Fig. 4 shows the DSC curves of the prepared NBR/AO-80 (100/40)a–c composites. The DSC curves of neat NBR and AO-80 (both as-received and quenched) are also included for comparison purposes. As shown in Fig. 4, the as-received AO-80 powder was crystalline and had the melting temperature at around 122.5 °C, and the neat NBR had a glass transition temperature at around −16 °C. After the as-received AO-80 was heated to 160 °C and quickly quenched to room temperature, amorphous AO-80 with a glass transition temperature at around 40.9 °C was obtained. The DSC curve of the NBR/AO-80 (100/40)a composite showed both the melting temperature of AO-80 and the glass transition temperature of NBR, indicating that the AO-80/NBR interactions in the composite were weak. This further supports the previous conclusion that the NBR/AO-80a composites were micro-composites and not nanocomposites. The DSC curve of the NBR/AO-80 (100/40)b composite, however, shows neither the melting peak nor the glass transition peak of AO-80, and the glass transition temperature of NBR was shifted from −15.9 °C to −2.1 °C. This further supports the previous discussion that the NBR/AO-80b composites could be molecular composites. Intriguingly, the DSC curve of the NBR/AO-80 (100/40)c composite also shows neither the melting peak nor the glass transition peak of AO-80, and the glass transition temperature of NBR was further shifted from −2.1 °C to 2.5 °C. This led us to believe that the re-generated AO-80 nanoparticles actually contained some NBR chain segments, and the NBR matrix also contained some molecularly dispersed AO-80. In other words, the NBR/AO-80 (100/40)c composite had two phases: (1) the AO-80 enriched phase (nanoparticles) and (2) the NBR enriched phase (matrix).

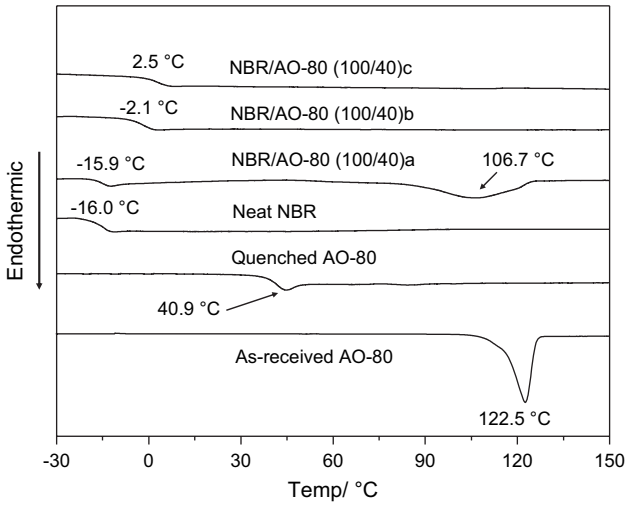

Fig. 4. DSC curves of AO-80 (as-received and quenched), neat NBR and NBR/AO-80 (100/40) composites.

Fig. 5 shows the X-ray diffraction (XRD) traces of the NBR/AO-80 (100/40) composites in different preparation stages, as well as the XRD traces of AO-80 (both as-received and quenched) and neat NBR. As shown in Fig. 5, the as-received and quenched AO-80 demonstrate typical crystalline and amorphous characteristics, respectively. The XRD trace of the NBR/AO-80 (100/40)a composite was similar to that of the as-received AO-80, indicating that the AO-80 in the NBR/AO-80 (100/40)a composite was in the crystalline form. The XRD traces of the NBR/AO-80 (100/40)b and c composites, however, indicated that AO-80 in both composites were amorphous. Overall, the XRD results were consistent with the DSC results, and further supported the above conclusions.

FT-IR/ATR is a powerful tool to investigate the interactions among functional groups. Fig. 6 shows the FT-IR/ATR spectra of the quenched AO-80 and the NBR/AO-80 (100/60)c nanocomposites. In the AO-80 spectrum, the infrared band centered at 3484.9 cm^{-1} was associated with the hydrogen-bonded hydroxyl group. The infrared band for the non-hydrogen-bonded hydroxyl group was located at around 3606.9 cm^{-1}. As shown in Fig. 6, hydroxyl groups in the quenched AO-80 were primarily hydrogen bonded; the amount of non-hydrogen-bonded hydroxyl groups (barely seen as a shoulder in the spectrum) was very limited. On the other hand, the amount of non-hydrogen-bonded hydroxyl groups increased significantly in the spectrum of the NBR/AO-80 (100/60)c composite. This was because AO-80 formed nano-scaled particles (average size of approximately 20 nm) in the NBR/AO-80 (100/60)c composite, thus the percentage of surface hydroxyl groups was much higher than that in the quenched AO-80. These hydroxyl groups on the surface of nanoparticles were non-hydrogen bonded because they strongly interacted with the nitrile groups of NBR in the matrix. The other band centered at 3473.1 cm^{-1} was assigned to the hydroxyl groups inside the nanoparticles.

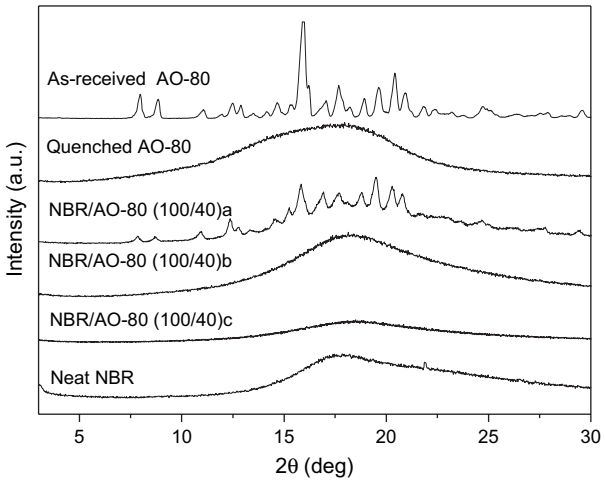

Fig. 5. XRD spectra of AO-80 (as-received and quenched), neat NBR and NBR/AO-80 (100/40) composites.

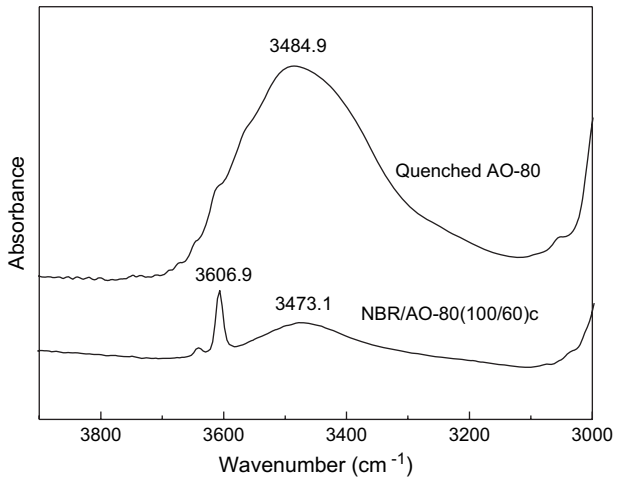

Fig. 6. FT-IR/ATR spectra of the quenched AO-80 and NBR/AO-80 (100/60)c nanocomposites.

3.3. Dynamic mechanical property of NBR/AO-80c nanocomposites

Fig. 7 shows the temperature dependence of the loss tangent (tan δ) values of the prepared NBR/AO-80c nanocomposites with various mass ratios of NBR/AO-80. Fig. 7 indicates that all of the NBR/AO-80c nanocomposites had only one tan δ peak. With an increasing amount of AO-80 in the nanocomposites, the tan δ peak gradually shifted to higher temperatures and the peak also became broader. Specifically, when the AO-80 amount in the nanocomposites increased from 0 phr to 100 phr, the tan δ value increased from 1.9 to 3.2. Such an uncommon but favorable increase in the tan δ value was very interesting. It is well known that the damping performance of a polymeric material is determined mainly by its viscoelastic behavior in a transitional region between the glassy and the rubbery states (near the glass transition temperature). In this region, macromolecular chain segments, but not entire macromolecules, tend to vibrate in phase with an external

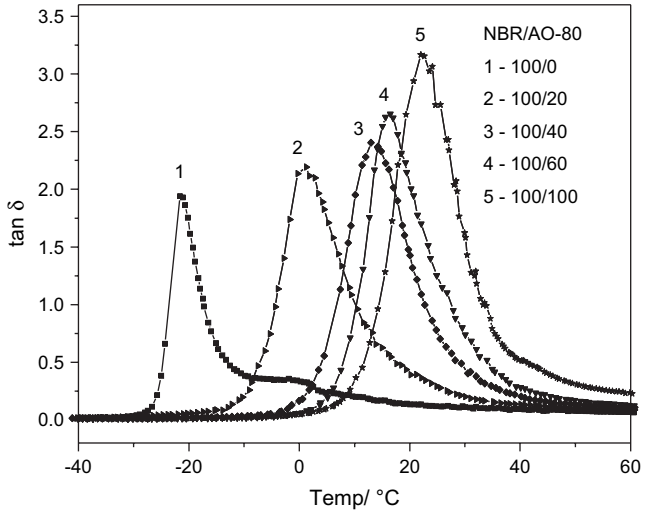

Fig. 7. Temperature dependence of the loss tangent (tan δ) values for NBR and NBR/AO-80c nanocomposites with varied mass ratios of NBR/AO-80.

vibration. However, molecular conformation changes usually cannot keep up with the imposed vibration, resulting in internal friction and energy dissipation [14]. The stronger the internal friction, the higher the tan δ value and the better the damping performance of the material will be. Generally speaking, the introduction of inorganic fillers (such as carbon black, silica and metal oxide/hydroxide) [15] and/or organic molecules (such as plasticizers) [16] into a polymer typically leads to a decrease of the tan δ value, because the interactions between the filler and the matrix are often weak. For the NBR/AO-80c nanocomposites, however, the strong intermolecular interactions between AO-80 and NBR reduced the mobility of NBR chain segments and caused the high energy dissipation under dynamic deformations; this results in an increase of the tan δ value. Additionally, the broadening of the tan δ peaks with the increasing of AO-80 amounts suggests that numerous types of interactions existed in the NBR/AO-80c nanocomposites. These interactions included the interactions between AO-80 and NBR in the AO-80 enriched phase (nanoparticles) and in the NBR enriched phase (matrix), the interfacial interaction between nanoparticles and matrix, as well as the interaction among AO-80 molecules and among NBR molecules (including chemical and topological entanglements) and others. Taken together, high tan δ values and broad transition temperature ranges suggest that the NBR/AO-80c nanocomposites could possess excellent damping properties.

Fig. 8 shows the temperature dependence of the storage moduli (E') of the prepared NBR/AO-80c nanocomposites. All of the storage modulus curves displayed only one transition, and the curves gradually moved toward higher temperatures with an increase in the amount of AO-80. Unlike the situation in the rubber nanocomposites containing inorganic fillers (in which E' values always increased with increasing the filler amount [15]), the E' values in the glassy regions of the NBR/AO-80c nanocomposites did not vary significantly, whereas the E' values in the rubbery regions decreased, as the amount of AO-80 increased. This was because the stiffness of AO-80 enriched phase (nanoparticles) was similar to that of the crosslinked NBR matrix; therefore the AO-80 nanoparticles had little effect on the nanocomposites' E' values when the nanocomposites were in the glassy state. When the nanocomposites were in the rubbery state, especially when the temperature was higher than the glass transition temperature of AO-80 (40.9 °C), the AO-80 nanoparticles became soft and acted as a plasticizer, and the E' values decreased.

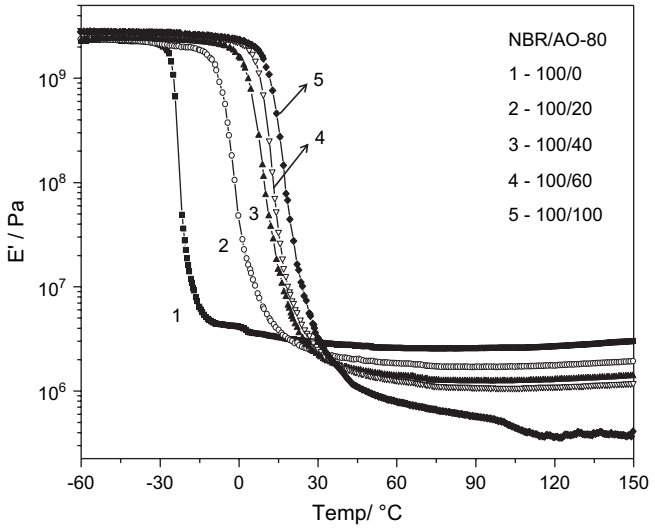

Fig. 8. Temperature dependence of the storage modulus (E') for NBR and NBR/AO-80c nanocomposites with varied mass ratios of NBR/AO-80.

3.4. Static mechanical property of NBR/AO-80c nanocomposites

Fig. 9 shows the tensile stress/strain curves of the prepared NBR/AO-80c nanocomposites with various NBR/AO-80 mass ratios, and Table 1 summarizes the acquired data. The tensile strength and elongation at break of the crosslinked neat NBR (NBR/AO-80(100/0)) were 3.1 MPa and 373%, respectively. These values were low but reasonable because no reinforcement agent (AO-80) was added. The uncrosslinked NBR/AO-80 (100/40) composite showed extremely low strength but very large elongation at break. This was because the NBR molecules in the uncrosslinked composite could slide under tension. As expected, crosslinking had a significant impact on the tensile strength. As shown in Table 1, all of the crosslinked composites had much higher tensile strength, particularly the ones containing AO-80. The tensile strength of the NBR/AO-80 (100/60)c nanocomposite exceeded 17 MPa,

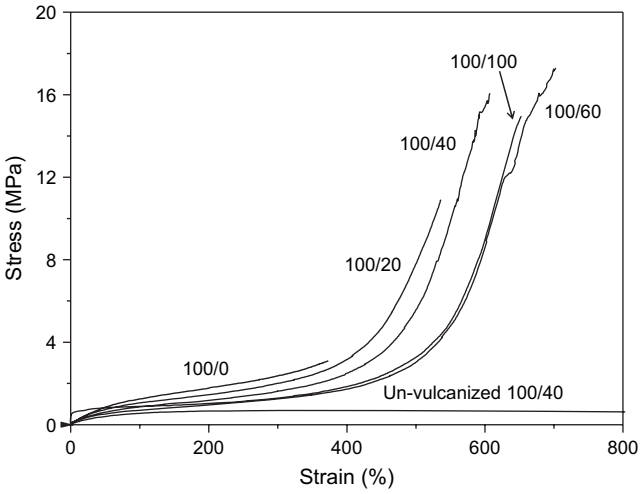

Fig. 9. Stress/strain curves of NBR and NBR/AO-80c nanocomposites with varied mass ratios of NBR/AO-80.

Table 1
Mechanical properties of NBR/AO-80c nanocomposites

Properties	Loadings of AO-80					
	0 phr	20 phr	40 phr	60 phr	100 phr	40 phr[a]
Hardness (Shore A)	59	57	63	75	88	–
Tensile strength (MPa)	3.1	10.9	16.0	17.3	15.0	0.6
Elongation at break (%)	373	536	608	703	653	1100
Permanent set (%)	4	4	6	6	8	>100

[a] Uncrosslinked nanocomposites.

which was 5–6 times higher than that of the crosslinked neat NBR. As discussed in Section 1, when fillers were distributed in rubber matrices as nano-sized particles and the interfacial bonding was reasonably strong, an effective reinforcement would be achieved, and the nanocomposites would possess significantly improved tensile properties. Table 1 also lists the permanent set property of the NBR/AO-80c nanocomposites. The results indicated that the nanocomposites had very small permanent residual deformations, which is very important for applications.

3.5. Stability of NBR/AO-80c nanocomposites

This part of the research was conducted to evaluate the stability of the prepared NBR/AO-80c nanocomposites. Fig. 10 shows the DSC curves of the NBR/AO-80 (100/60)c nanocomposite after being annealed at 100 °C for varied periods of time. The results indicate that annealing did not cause any obvious change except a slight shift of NBR's glass transition temperature. Neither crystallization nor glass transition associated with AO-80 was identified. The slight increase of NBR's glass transition temperature was probably due to the continuous crosslinking/vulcanization of NBR during annealing. Fig. 10 indicates that the morphology and structure of the NBR/AO-80c nanocomposites were reasonably stable, even at an elevated temperature of 100 °C. In comparison, the annealing of the CPE/AO-80 composites at 100 °C caused AO-80 to phase separate and crystallize [17]. The difference of the stability between NBR/AO-80c nanocomposites and CPE/AO-80 composites is attributed to the formation of three-dimensional NBR networks, which could partially block the dispersed AO-80 molecules/nanoparticles and prevent them from aggregation into large particles during the annealing process.

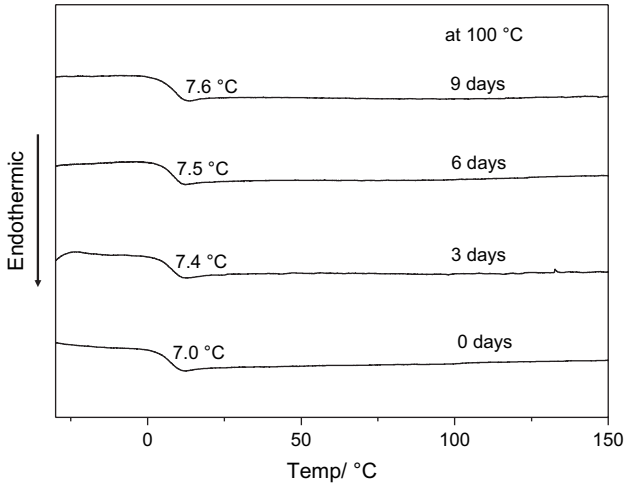

Fig. 10. DSC curves of NBR/AO-80 (100/60)c nanocomposites after being annealed at 100 °C for varied periods of time.

4. Conclusions

NBR/AO-80 rubber nanocomposites were successfully prepared in this study. The nanocomposites consisted of two phases: (1) the AO-80 enriched phase (nanoparticles with the average size of approximately 20 nm) and (2) the NBR enriched phase (matrix). The generation and uniform distribution of the nanoparticles are attributed to the high temperature mechanical kneading process, the strong intermolecular interactions between AO-80 and NBR molecules, and the formation of a three-dimensional NBR network. The morphological, structural and mechanical properties of the NBR/AO-80 rubber composites in each preparation step were systematically investigated. The results indicate that the prepared NBR/AO-80 rubber nanocomposites exhibited single relaxation transitions, improved tensile strengths, high dynamic mechanical loss values, and reasonably good stabilities. Therefore, the NBR/AO-80 rubber nanocomposites are expected to have important applications as a high performance damping material.

Acknowledgements

This work was supported by the National Nature Science Foundation of China (50403029). H.F. and M.T. would also like to thank the "Center for Accelerated Applications at the Nanoscale (CAAN)" at the South Dakota School of Mines and Technology (SDSM&T). The authors are grateful to Mr. Nyle E. Hedin for proofreading the manuscript.

References

[1] Hamed GR. Rubber Chem Technol 2000;73:524–33.
[2] Jia Q, Wu Y, Xu Y, Mao H, Zhang L. Macromol Mater Eng 2006;291:218–26.
[3] Zhang L, Wang Y, Wang Y, Sui Y, Yu D. J Appl Polym Sci 2000;78:1873–8.
[4] Ma J, Xiang P, Mai Y, Zhang L. Macromol Rapid Commun 2004;25:1692–6.
[5] Karger-Kocsis J, Wu C. Polym Eng Sci 2004;44:1083–93.
[6] Zhang Q, Tian M, Wu Y, Lin G, Zhang L. J Appl Polym Sci 2004;94:2341–6.
[7] Reichert WF, Goritz D, Duschi EJ. Polymer 1993;34:1216–21.
[8] Kilian HG, Strauss M, Hamm W. Rubber Chem Technol 1994;67:1–16.
[9] Wu Y, Jia Q, Yu D, Zhang L. Polym Test 2004;23:903–9.
[10] Wu C. J Non-Cryst Solids 1994;315:321–4.
[11] Wu C, Yamagishi T, Nakamoto Y, Ishida S, Nitta K, Kubota S. J Polym Sci Part B Polym Phys 2000;38:2285–95.
[12] Wu C, Otani Y, Namiki N, Emi H, Nitta K, Kubota S. J Appl Polym Sci 2001;82:1788–93.
[13] Wu C, Akiyama S. Polym Int 2003;52:1249–55.
[14] Sperling LH, Fay JJ. Polym Adv Technol 1991;2:49–56.
[15] Pattanawanidchai S, Saeoui P, Sirisinha C. J Appl Polym Sci 2005;96:2218–24.
[16] Kalkar K, Parkhi PS. J Appl Polym Sci 1995;57:233–43.
[17] Wu C, Akiyama S. J Polym Sci Part B Polym Phys 2004;42:209–15.